

REGENERATIVE AMPLIFIER FEL – FROM IR TO X-RAYS

D. C. Nguyen†, P. M. Anisimov, C. E. Buechler, Q. R. Marksteiner, R. L. Sheffield
 Los Alamos National Laboratory, Los Alamos, New Mexico, USA

Abstract

The Regenerative Amplifier FEL (RAFEL) feeds back a small fraction of the radiation exiting a high-gain undulator as the seed for the next pass, and achieves narrow linewidth and saturation in a few passes. For the IR RAFEL, we used an optical cavity with annular mirrors to reinject ~10% of the IR radiation back into a two-meter undulator [1]. We theorized the RAFEL output transformed from an annular beam to an on-axis beam due to optical guiding at high power [2]. A number of researchers have proposed RAFEL and XFEL to achieve full temporal coherence in VUV and X-ray FELs [3-8]. For the XFEL, symmetric Bragg backscattering off high-quality diamond crystals can provide very high reflectivity for the XFEL cavity [7-9]. The required reflectivity for a RAFEL feedback cavity is much lower than the XFEL. We show that 6% feedback is sufficient for the X-ray RAFEL at 9.8 keV to saturate and achieve 0.5-eV bandwidth. We discuss options to out-couple more than ~50% of the RAFEL intra-cavity power and discuss challenges associated with X-ray absorption in the out-coupler.

INTRODUCTION

With the successful commissioning of the European XFEL and the on-going construction of the LCLS-II superconducting linac XFEL at SLAC, a fully coherent X-ray free-electron laser delivering transform-limited X-ray pulses with unprecedented brilliance is a real possibility in the near future. Full temporal coherence can be achieved with either an XFEL or an X-ray RAFEL, both of which will require an optical cavity consisting of low-loss, high-quality Bragg mirrors [10]. The XFEL requirements for are more stringent: Bragg crystals with 99% reflectivity forming a long optical cavity with μm dimension accuracy and nanoradian angular stability, in addition to the relatively long and high charge electron bunches at MHz bunch repetition rate. Numerical simulations predict the X-ray pulses inside an XFEL optical cavity will need to recirculate a few hundred passes before they reach steady-state and achieve narrow linewidth [9]. In contrast, the RAFEL requires 2-3 passes in a lower-Q feedback cavity (lower reflectivity) and less stringent angular stability compared to the XFEL. The RAFEL has been demonstrated in the infrared by our group [1] and proposed by a number of researchers for the VUV and X-ray regions as a means to generate fully coherent short-wavelength FELs [3-8].

The RAFEL design shares a number of features of the XFEL such as improved longitudinal coherence and pulse-to-pulse stability over SASE. There are however a few important differences between RAFEL and XFEL.

First and foremost is the amount of optical feedback in each pass; in RAFEL, the optical feedback is typically a few percent of radiation power in the previous pass, whereas XFEL requires feedback fraction greater than 90%. Thus, while the intra-cavity power of the XFEL is several times the output power, the RAFEL output power is almost the same as the power exiting the undulator. The small optical feedback in RAFEL significantly relaxes the reflectivity requirements for the cavity mirrors. The second difference is the single-pass gain; the RAFEL single-pass gain is high, on the order of 10^2 to 10^3 , compared to the XFEL single-pass gain of ~2X. The higher gains reduce the number of passes for RAFEL to reach saturation and achieve spectral narrowing. The third difference is the output spectral width; the XFEL can achieve a very narrow linewidth (a few meV) whereas the RAFEL output has a spectral width of a single SASE spectral peak, which is approximately the Fourier transform of the X-ray pulse width (about the same as the electron bunch length).

We present experimental results of the IR RAFEL and numerical simulations of a fully coherent RAFEL at 9.8 keV with spectral linewidth of ~0.5 eV (5×10^{-5} relative). We show candidates for the low-loss Bragg reflectors for different X-ray energies, discuss a number of options to out-couple the intra-cavity power and present the results of Genesis FEL simulation for the 9.8-keV RAFEL.

INFRARED RAFEL

The infrared RAFEL was experimentally demonstrated at 16 μm at LANL in 1997. The feedback cavity for this demonstration is shown in Fig. 1. The electron beam entered the cavity from the left through the smaller annular mirror and exit on the right. Approximately two-third of the intra-cavity power was coupled out through the large annular mirror. A summary of the IR RAFEL parameters is shown in Table 1.

Table 1: Summary of IR RAFEL Parameters

Parameter	Symbol	Value
Beam energy	E_b	16.7 MeV
Peak current	I_p	270 A
Bunch length	l_c	5 mm
Undulator period	λ_u	2 cm
Undulator parameter	K_{rms}	0.92
Undulator length	L_u	2 m (1 m taper)
FEL wavelength	λ	16.3 μm
3D gain length	L_G	0.125 m

† dcnguyen@lanl.gov

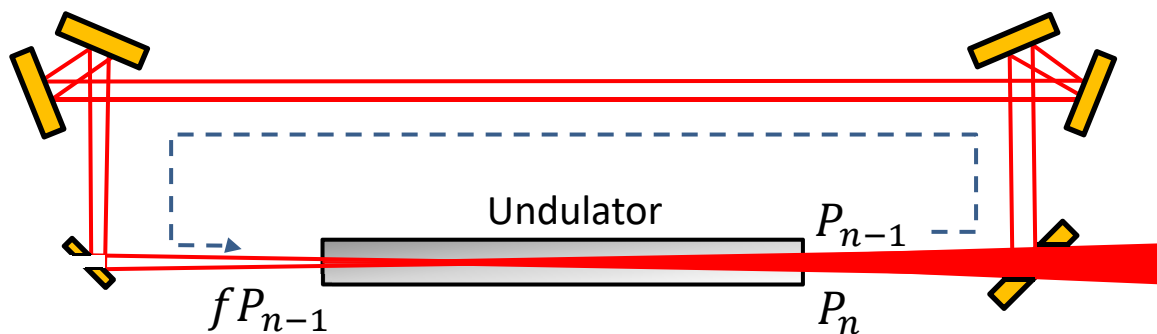


Figure 1: Schematic of the IR RAFEL. The optical feedback cavity consists of six copper mirrors, two flat annular mirrors and two pairs of curved mirrors. The electron beam travels from the left through the two annular mirrors and the undulator.

The pairs of mirrors at the top of Fig. 1 form two off-axis paraboids; one paraboloid collimates the diverging IR beam and the other focuses the IR beam to a small waist at a location about 2 gain lengths inside the undulator. The first annular mirror on the left has a 5-mm diameter hole to allow most of electron beam to pass through and enter the undulator. The second annular mirror on the right has a 14-mm diameter hole to allow the electron and two-third of the FEL power to exit. We estimate only 10% of the IR beam is reinjected into the undulator. Two sets of IR pulses circulate in the feedback cavity that has a roundtrip time of 18.46 ns, twice the electron bunch separation of 9.32 ns. The RAFEL power at the end of the n^{th} pass is given by

$$P_n = (fP_{n-1}) \frac{1}{9} e^{\frac{L_u}{L_G}}$$

where f is the feedback fraction, L_u is the undulator length and L_G is the 3D gain length. Fig. 2 shows the optical power build-up from noise to saturation. The net gain per pass is about 1.5X. From the cavity ring-down (Fig. 3), we deduce a cavity loss per pass of ~66%. Thus, we estimate the RAFEL has a large-signal gain of 4.5X. The calculated small-signal gain is much higher, about 330X per pass.

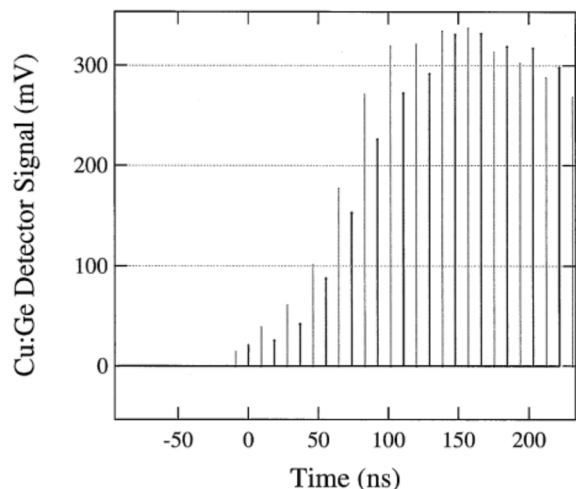


Figure 2: Optical energy build-up in the IR RAFEL. Two sets of IR pulses (dark and gray) exist inside the ring cavity with round-trip time twice the electron bunch spacing.

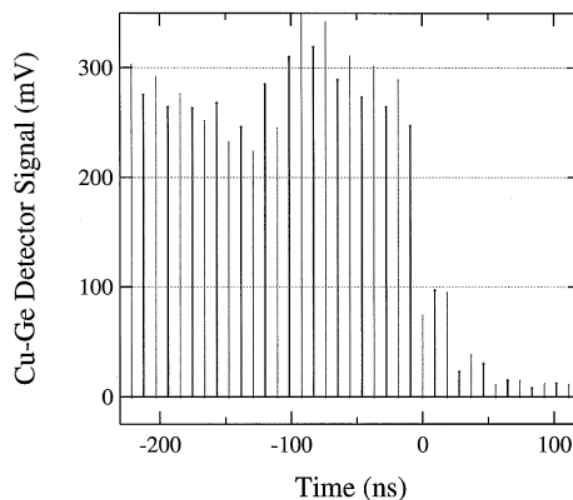


Figure 3: Ring-down of the IR RAFEL energy. The pulse energy decreases to one-third its initial value in one pass.

We measured the output energy of ~1,000 micropulses versus detuning from the synchronous cavity length. The cavity length detuning FWHM is 1 mm (Fig. 4), approximately the electron bunch length (5 mm) divided by the number of passes (~6) for the FEL pulse to saturate.

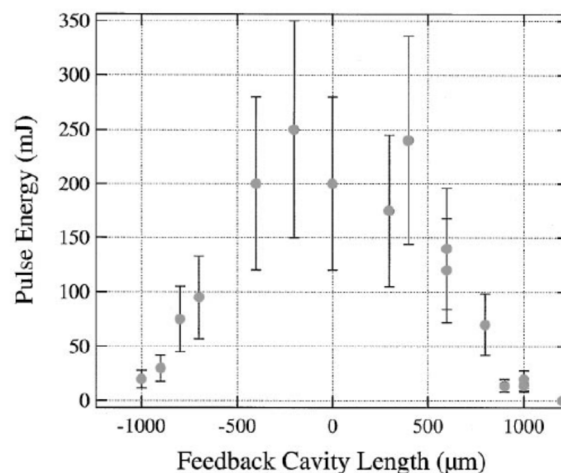


Figure 4: Cavity detuning length of the IR RAFEL.

X-RAY RAFEL WITH BRAGG MIRRORS

Symmetric Bragg 45° Reflectors

The optical cavity will be for the X-ray RAFEL is likely to consist of four 45° high-quality diamond Bragg crystal reflectors, in the form of diamond drumheads that have been fabricated at Argonne National Laboratory [10]. The rectangular cavity is preferred due to the long and narrow shape of the undulator hall and the ease of installing evacuated beam pipe for the X-ray transport. The choice of 45° Bragg angle limits the RAFEL to a single X-ray energy for each Bragg crystal. Table 2 lists a few of the diamond crystals together with the inter-planar spacing, extinction length [11] and the X-ray energy where each of these diamond crystals can serve as 45° Bragg reflectors.

Table 2: Diamond 45° Bragg Reflectors for RAFEL

Diamond	d (Å)	Λ_H (μm)	Energy (keV)
(111)	2.0593	1.09	4.2573
(220)	1.2611	1.98	6.9521
(311)	1.0754	3.74	8.1521
(400)	0.8917	3.63	9.8318
(331)	0.8183	5.89	10.714
(422)	0.7281	5.03	12.0414
(333)	0.6864	7.83	12.7719
(531)	0.6029	9.82	14.5414

The Bragg reflectors operate over a very narrow angular cone, typically about 10 μrad FWHM and displaced from the Bragg angle by a small angle (Fig. 5). The peak reflectivity can be 99%, much higher than what the RAFEL needs. Due to the large single-pass gain, we will need to increase the transmission (and thus reduce the Bragg reflectivity) of one of the cavity reflectors in order to out-couple a large fraction of the intra-cavity power.

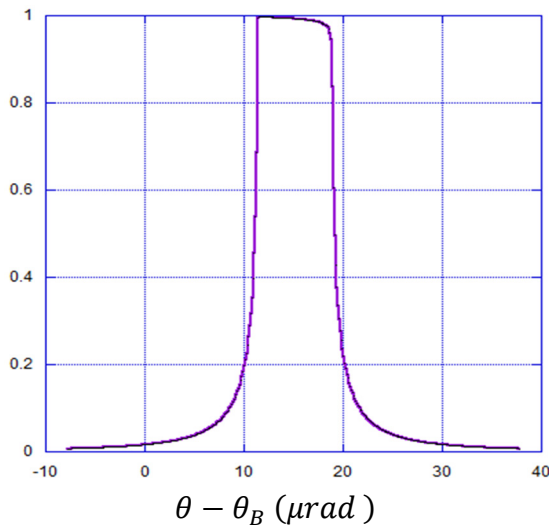


Figure 5: Calculated rocking curve for diamond (400).

Options for RAFEL Power Out-coupler

We present below four options for increasing the transmission of the Bragg out-coupler using thin diamond drumheads [10]:

Thin crystal out-coupling Higher transmission is accomplished by selecting a Bragg crystal thickness to be on the order of the extinction length, defined as the depth in the Bragg crystal where the radiation intensity decreases to 1/e of the radiation intensity at the Bragg crystal surface. The symmetric Bragg reflectivity scales linearly with the thickness in the range of the crystal thickness that is approximately one extinction length.

Tilted Bragg out-coupling Higher transmission can be obtained by tilting the Bragg out-coupler by a small angle $\delta\theta$. Since the cavity reflectors are aligned to a very small angular acceptance, the tilted Bragg crystal will have a lower reflectivity as determined by the cavity angle.

Heated Bragg out-coupling Higher transmission can be obtained by heating the Bragg out-coupler, effectively shifting the Bragg condition to a lower X-ray energy by a small deviation δE . Since the cavity reflectors are aligned to a very narrow range of energy (blue line), the shifted Bragg condition will have lower reflectivity (Fig. 6).

Pinhole Bragg out-coupling Higher transmission can be obtained by drilling a pinhole in the Bragg crystal. Hole-coupling has worked in the visible and infrared. Pinhole outcoupling has been proposed for X-ray RAFEL [12].

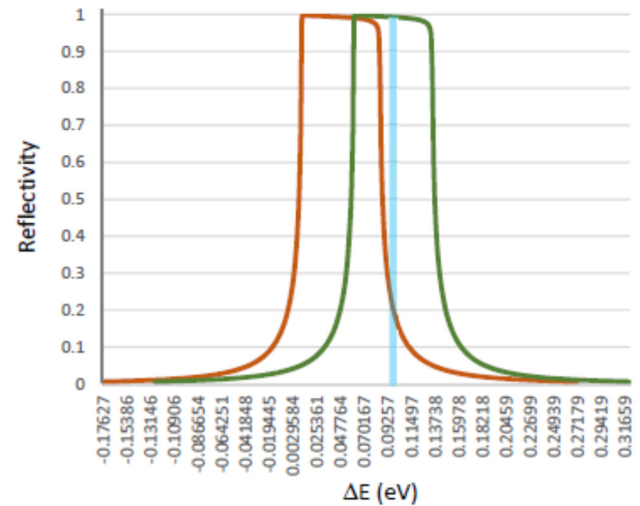


Figure 6: Reflectivity versus energy detuning from Bragg for diamond (400) at 20°C (green) and 45° (orange).

Figure 7 illustrates a possible X-ray RAFEL optical cavity with four Bragg reflectors forming a rectangular cavity. The diverging X-ray beam exiting the undulator is collimated by a compound refractive lens (CRL) and focused to a waist near the undulator entrance by the other CRL. The upper-right reflector R_1 serves as the out-coupler.

Content from this work may be used under the terms of the CC BY 3.0 licence (© 2019). Any distribution of this work must maintain attribution to the author(s), title of the work, publisher, and DOI

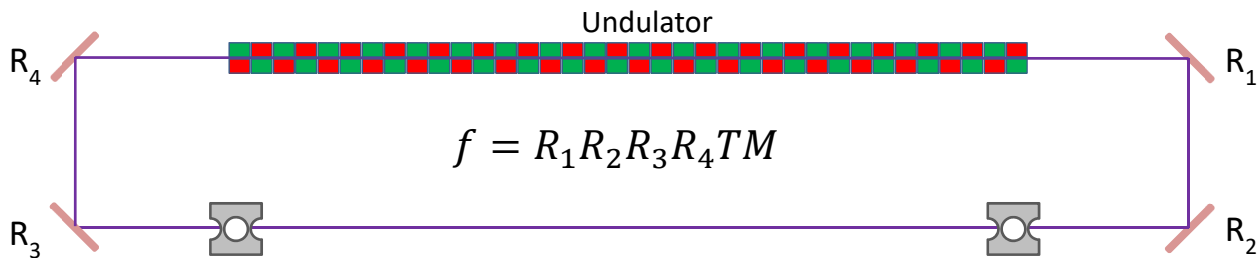


Figure 7: Schematic of an X-ray RAFEL. The feedback fraction f is the product of the four mirror reflectivity (R_1 through R_4), the combined transmission T of the two compound refractive lenses (CRL) and the spectral power fraction selected by the Bragg mirrors M within the cavity angular acceptance as defined by the radiation mode over the CRL separation.

X-RAY RAFEL GENESIS SIMULATIONS

We performed time-dependent FEL simulations using the Genesis 1.3 FEL simulation code [12]. The parameters for the electron beam and RAFEL optical feedback are summarized in Table 3.

Table 3: Summary of X-ray RAFEL Parameters

Parameter	Symbol	Value
Beam energy	E_b	10.5 GeV
Peak current	I_p	2.5 kA
Bunch length	l_e	2.4 μm
Bunch charge	q	20 pC
Norm. rms emittance	ε_n	0.2 μm
rms energy spread	δE_b	1.05 MeV
Undulator period	λ_u	2.6 cm
Undulator parameter	K_{rms}	1.76
Undulator length	L_u	3.38 m
# of undulators	N_u	7
FEL wavelength	λ	1.261 \AA
FEL gain parameter	ρ	0.001
3D gain length	L_G	1.37 m

The number of undulators used in these simulations (seven) is chosen such that the SASE radiation has a well-defined transverse mode and the SASE power is sufficiently high so that only 6% feedback ($f = 0.06$) within the spectral and angular width of the cavity mirrors far exceeds the start-up noise. The cavity angular width is defined by

$$\Delta\theta \sim \frac{w_r}{L}$$

where w_r is the radiation mode $1/e^2$ radius on the CRL and L is the distance between the CRLs.

Figure 8 show the semi-log plots of SASE power (blue), RAFEL power in Pass 2 (orange), Pass 3 (yellow), Pass 4 (green) and Pass 5 (purple). The SASE power is simulated with more than seven undulators to show the saturated SASE power; however, only seven undulators are used in the simulations of SASE power with the narrow spectral

filter. The RAFEL power growth curves show lethargy and synchrotron oscillation typical of coherent amplification.

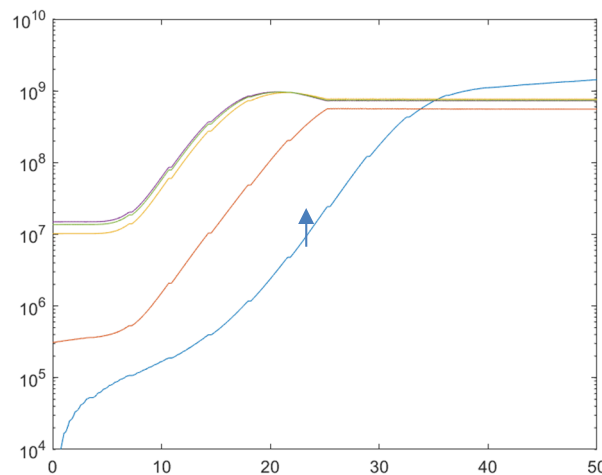


Figure 8: Semi-log plots of SASE (blue), pass 2 (orange), pass 3 (yellow), pass 4 (green) and pass 5 (purple). The SASE simulation is stopped at the 7th undulator (arrow).

Figure 9 plots the SASE and filter spectra on a linear scale, showing only 6% of the power within a SASE spectral spike (orange) is used as the coherent seed for Pass 2.

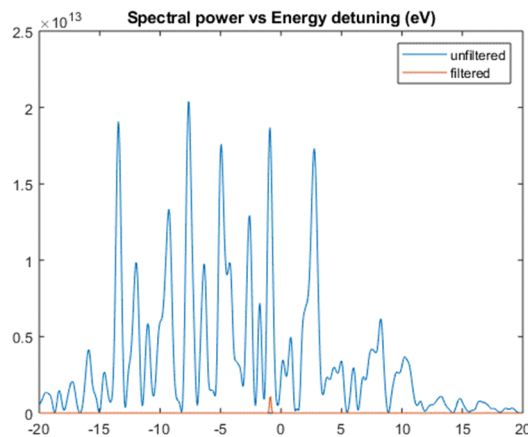


Figure 9: SASE and filtered signal on a linear scale. The Gaussian-shaped filter selects only 6% of the spectral power within a single SASE spike as the coherent seed for amplification in Pass 2.

In Fig. 10, we show the RAFEL spectrum at the end of the 7th undulator on the linear (10a) and log (10b) scales. The spectral width of the RAFEL peak in Pass 5 is 0.5 eV, wider than the spectral width of the filter (0.15 eV). The RAFEL spectral width is determined by the Fourier transform of the short electron bunch and not by the Bragg spectral width. An interesting result is the suppression of SASE by two orders of magnitude in Pass 5 relative to Pass 1 (SASE only, no RAFEL). Since the RAFEL spectral power is enhanced by three orders of magnitude, the ratio of RAFEL to SASE in Pass 5 is five orders of magnitude.

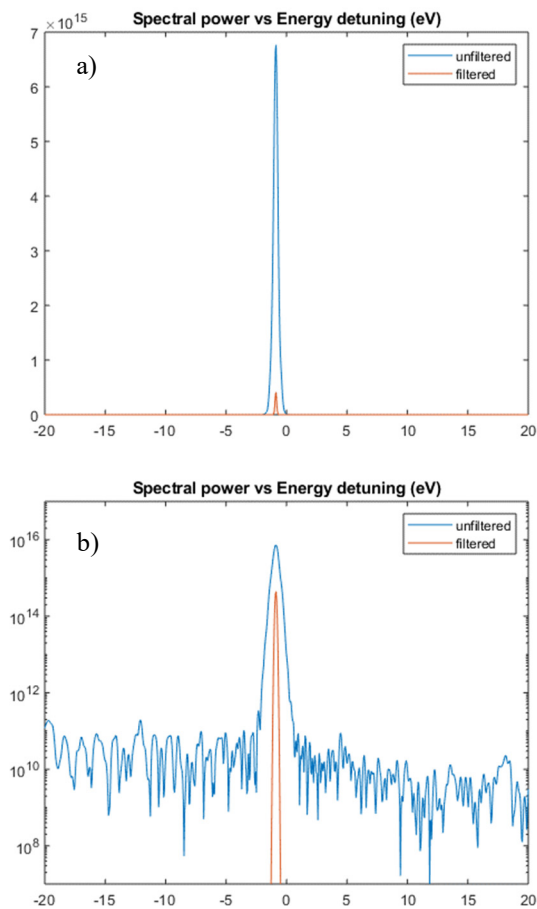


Figure 10: Plots of spectral power in Pass 5 versus energy detuning in eV on linear (a) and log (b) scale.

CONCLUSION

We have shown that the RAFEL with 45° diamond Bragg reflectors is a feasible approach to a fully coherent X-ray FEL with narrow linewidth. The spectral linewidth of a 9.83-keV X-ray RAFEL at saturation in Pass 5 is 0.5 eV, corresponding to 5×10^{-5} relative linewidth. Genesis simulations show that the X-ray RAFEL can saturate in two passes with only 6% feedback within the SASE spectral peak. While the total RAFEL power is slightly lower than the total SASE power, the RAFEL spectral brightness is three orders of magnitude higher than SASE. We observe a factor of 100X reduction in the SASE spectral power

when RAFEL is lasing, and thus the contrast between the coherent RAFEL spectral peak to the SASE background is five orders of magnitude.

ACKNOWLEDGEMENTS

We thank Yuri Shvyd'ko, Gabriel Marcus, Zhirong Huang, Ryan Lindberg, Tor Raubenheimer and Dilling Zhu for many helpful discussions and suggestions.

REFERENCES

- [1] D. C. Nguyen et al., "First Lasing of the Regenerative Amplifier FEL," *Nucl. Instr. Meth. Phys. Res. A*, vol. 429, p. 125, 1999.
DOI: 10.1016/S0168-9002(99)00090-X
- [2] J. C. Goldstein, D. C. Nguyen and R. L. Sheffield, "Theoretical study of the design and performance of a high-gain, high-extraction-efficiency FEL oscillator," *Nucl. Instr. Meth. Phys. Res. A*, vol. 393, p. 137, 1997.
DOI: 10.1016/S0168-9002(97)00445-2
- [3] B. Faatz et al., "Regenerative FEL amplifier at the TESLA test facility at DESY," *Nucl. Instr. Meth. Phys. Res. A*, vol. 429, p. 424, 1999.
DOI: 10.1016/S0168-9002(99)00123-0
- [4] Z. Huang and R. D. Ruth, "Fully Coherent X-Ray Pulses from a Regenerative-Amplifier Free-Electron Laser," *Phys. Rev. Lett.* vol. 96, p. 144801, 2006.
DOI: 10.1103/PhysRevLett.96.144801
- [5] B. W. J. McNeil et al., "A design for the generation of temporally-coherent radiation pulses in the VUV and beyond by a self-seeding high-gain free electron laser amplifier," *New Journal of Physics*, vol. 9, p. 239, 2007.
DOI: 10.1088/1367-2630/9/7/239
- [6] G. Marcus et al., "X-Ray Regenerative Amplifier Free-Electron Laser Concepts For LCLS-II," in *Proc. 38th Int. Free-Electron Laser Conf.*, Santa Fe, New Mexico, USA, August 2017, paper MOP061, DOI: 10.18429/JACoW-FEL2017-MOP061
- [7] K.-J. Kim, Y. V. Shvyd'ko, and S. Reiche, "A Proposal for an X-Ray Free-Electron Laser Oscillator with an Energy-Recovery Linac," *Phys. Rev. Lett.* vol. 100, p. 244802, 2008.
DOI: 10.1103/PhysRevLett.100.244802
- [8] K.-J. Kim and Y. V. Shvyd'ko, "Tunable Optical Cavity for an X-ray Free-electron-laser Oscillator," *Phys. Rev. ST Accel. Beams*, vol. 12, p. 030703, 2009.
DOI: 10.1103/PhysRevSTAB.12.030703
- [9] R. R. Lindberg et al., "Performance of the X-ray Free-Electron Laser Oscillator with Crystal Cavity," *Phys. Rev. ST Accel. Beams*, vol. 14, p. 010701, 2011.
DOI: 10.1103/PhysRevSTAB.14.010701
- [10] T. Kolodzie et al., "Diamond Drumhead Crystals for X-ray Optics Applications," *J. Applied Crystallography*, vol. 49, pp. 1240–1244, 2016.
DOI: 10.1107/S1600576716009171
- [11] Y. Shvyd'ko and R. Lindberg, "Spatiotemporal response of crystals in x-ray Bragg diffraction," *Phys. Rev. ST Accel. Beams*, vol. 15, p. 100702, 2012.
DOI: 10.1103/PhysRevSTAB.15.100702
- [12] H. P. Freund, P. Van der Slot, Yu. Shvyd'ko, "An X-Ray Regenerative Amplifier Free-Electron Laser Using Diamond Pinhole Mirrors," arXiv:1905.06279 (2019)